Investigation of Dissipativity for Control of Smart Dampers via LMI Synthesis

Erik A. Johnson and Baris Erkus

Abstract—**This paper investigates the effects of dissipativity on the performance of semiactive systems with smart dampers via linear matrix inequality (LMI) methods. First, a linear quadratic regulator (LQR) problem is defined in terms of a linear objective function and several LMI constraints. Second, two dissipativity indices are proposed to quantify the dissipative nature of a force. One of the dissipativity indices is appended as an LMI constraint in its weak form to the LMI-LQR problem to exploit the dissipative nature of a smart damper. The dissipativity indices and the proposed controller are employed for a two-degree-of-freedom structure with a clipped optimal control problem. It is observed that the proposed method is able to improve the dissipative nature of the controller, improving the semiactive performance.**

I. Introduction

SMART dampers constitute an important class of semiactive devices used for structural control and vibration mitigation in civil engineering [1], [2]. These devices are controllable dampers and, therefore, they dissipate energy from the system to which they are attached. An often-used semiactive control strategy to command a smart damper is clipped optimal control [3]–[5], which employs a linear active control theory to design a primary controller assuming that the structure is linear and the control device is fully active, and a clipping algorithm as a secondary controller to make the damper produce a force close to that commanded by the primary controller (Fig. 1). The primary controller is generally a linear quadratic (LQ) optimal controller since this class of control theory is widely applied in structural control. It has been shown that a clipped optimal control strategy with a smart damper demonstrates results competitive to a corresponding active control strategy for most of the civil structures.

Manuscript received February 3, 2005. This work was supported in part by National Science Foundation under CAREER grant CMS 00-94030, and by the U.S. Department of Transportation through grant 03-17 from the National Center for Metropolitan Transportation Research (METRANS).

Erik A. Johnson is with Dept. of Civil and Enviromental Engineering, University of Southern California, CA 90089-2531 USA (phone: 213-740-0610; fax: 213-744-1426; e-mail: JohnsonE@usc.edu).

Baris Erkus is with Dept. of Civil and Enviromental Engineering, University of Southern California, CA 90089-2531 USA (e-mail: erkus@usc.edu).

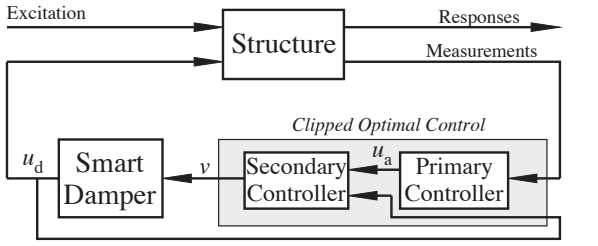

Fig. 1. A simplified representation of clipped optimal control strategy.

The effectiveness of a smart damper commanded by the clipped optimal control strategy can be explained by the primary control force being highly dissipative and, thus, suitable for the damper to mimic. For example, in some controlled structures, the damper can successfully mimic the primary control force due to high dissipativity of the force (*e.g.*, [3] and [6]), while for the other structures it cannot (*e.g.,* [4] and [6]). Although the dissipativity is an important concept in understanding the the performance of a semiactive system with a smart damper, there is very little work that investigates dissipativity due to the absence of well defined dissipativity indices. Inaudi [6] proposed a stochastic index that estimates the probability of the primary control force being dissipative, *i.e.,* $P[u_a v < 0]$. Simple deterministic indices based on dynamic time-history analyses are also used to observe the effect of the dissipative nature of the control force (*e.g.*, [4]).

Dissipativity indices — particularly stochastic indices — are important in the sense that they can be used in conjunction with special methods, such as linear matrix inequality (LMI) synthesis, to obtain controllers with various dissipativity levels. Although LMI methods are quite popular in the control field [7], they are rarely used in civil engineering applications (*e.g.*, [8]). The benefit of these methods is that they allow numerical solution of an optimal control problem with multiple objectives that does not have an analytical solution. In these methods, the control problem is represented in terms of bilinear and linear matrix inequalities (BMIs and LMIs). If the BMIs can further be represented in terms of LMIs, it can be solved by powerful numerical techniques [9] using available software. In this regard, convex multiobjective techniques can be used to investigate the effects of dissipativity on the performance of semiactive systems employing stochastic dissipativity indices.

This paper investigates the dissipativity and performance of semiactive systems by utilizing LMI methods to modify an LQR controller to achieve controllers with various dissipativity characteristics. First, a state-feedback LQR problem is represented as an optimization problem with convex LMIs. Then, available dissipativity indices are reviewed, and two indices are proposed. One of the indices is represented in its weak form as an LMI constraint and appended to the LQ problem. The modified LQR controller is implemented for a numerical example to observe the dissipativity–performance relations for several dissipativity levels and controller parameters. The numerical example is a two-degree-of-freedom shear structure (2DOF) with an ideal semiactive damper attached between the first and second stories. The results are presented in tabular and graphical forms. The MATLAB® LMI Control Toolbox [10] is used as the LMI solver.

II. LMI-EVP Representation of an LQR Problem

In this section, first, a method for the LMI characterization of a multiobjective optimization problem is summarized. Then, an LMI characterization of a standard linear quadratic regulator (LQR) problem is given. See [7] and [15] for fundamental notations and definitions used herein.

A. LMI Characterization of Multivariable Feedback Control Systems

A method for LMI characterization of multiobjective control problems is given by [20] and summarized here:

- Consider a closed-loop system $\dot{\mathbf{q}}_c = \mathbf{A}_c\mathbf{q}_c$, where $\mathbf{A}_c$ is Hurwitz. Let $\mathbf{S} = \mathbf{S}^T > 0$ satisfy the Lyapunov inequality $\mathbf{A}_c\mathbf{S} + \mathbf{S}\mathbf{A}_c^T + \mathbf{Q} < 0$ for the closed-loop system where $\mathbf{Q} = \mathbf{Q}^T > 0$.
- For each of the objectives, a matrix inequality condition, $\mathbf{F}_i(\mathbf{A}_c(\mathbf{K}), \mathbf{S}_i) > 0$ where $\mathbf{S}_i$ is the Lyapunov matrix of the i^{th} constraint and $\mathbf{K}$ is the controller, is found. These inequalities are, in general, BMIs.
- To enforce a unique Lyapunov matrix for the system, all the Lyapunov matrices are set to a single Lyapunov matrix as $\mathbf{S}_1 = \ldots = \mathbf{S}_N = \mathbf{S}$. Therefore, a problem with several BMIs, whose Lyapunov matrices are all $\mathbf{S}$, is obtained.
- Using new variables and some algebra, BMIs are converted into LMIs. The final problem has convex LMI constraints and can be solved numerically. Note that the mapping between the BMIs and LMIs must be one-to-one.
- If the problem includes an optimization criteria, the LMI problem is generally in the form of an eigenvalue problem (EVP) [7]. The representation of an eigenvalue problem that will be employed in this paper is as follows:

$$\min_{\mathbf{x}} \mathbf{c}^T\mathbf{x}, \qquad \text{subject to } \mathbf{F}(\mathbf{x}) > 0 \tag{1}$$

where $\mathbf{c}$ is a known vector and $\mathbf{F}(\mathbf{x}) > 0$ is an LMI.

B. LQR Control Problem

Consider a linear time-invariant system:

$$\begin{aligned} \dot{\mathbf{q}} &= \mathbf{A}\mathbf{q} + \mathbf{B}\mathbf{u} + \mathbf{E}\mathbf{w} \\ \mathbf{z} &= \mathbf{C}_z\mathbf{q} + \mathbf{D}_z\mathbf{u} + \mathbf{F}_z\mathbf{w} \end{aligned} \tag{2}$$

where $\mathbf{q}$ is the state vector, $\mathbf{u}$ is a vector of control forces, $\mathbf{w}$ is a stationary zero-mean white noise stochastic vector process disturbance with unit intensity, and $\mathbf{z}$ is the vector of outputs to be minimized. In structural control, the excitation and the outputs are selected such that $\mathbf{F}_z$ is zero. The LQR problem is to find the constant feedback gain $\mathbf{K}$ that satisfies the optimization

$$\begin{aligned} &\min_{\mathbf{K}} E[\mathbf{q}^T\mathbf{Q}\mathbf{q} + \mathbf{u}^T\mathbf{R}\mathbf{u} + \mathbf{q}^T\mathbf{N}\mathbf{u} + \mathbf{u}^T\mathbf{N}^T\mathbf{q}] \\ &\text{subject to } \dot{\mathbf{q}} = \mathbf{A}\mathbf{q} + \mathbf{B}\mathbf{u} + \mathbf{E}\mathbf{w}, \quad \mathbf{u} = -\mathbf{K}\mathbf{q} \end{aligned} \tag{3}$$

where $\mathbf{Q} = \mathbf{Q}^T \geq 0$, $\mathbf{R} = \mathbf{R}^T > 0$ and $\mathbf{N}$ are weighting matrices that must satisfy

$$\mathbf{W} = \begin{bmatrix} \mathbf{Q} & \mathbf{N} \\ \mathbf{N}^T & \mathbf{R} \end{bmatrix} \geq 0 \text{ and } \mathbf{R} > 0 \tag{4}$$

to have a well-posed LQR problem.

C. LMI-EVP Representation of an LQR Problem

A derivation of the LMI-EVP representation of an LQR problem is summarized utilizing the aforementioned method. There is a vast body of literature on LMI characterization of control systems; the method presented below is not the only way to obtain an LMI representation of an LQR problem. Some important works are [16]–[20].

The LQR problem is redefined in a form suitable for LMI characterization as follows: Let $\mathbf{Q}^{1/2}$ and $\mathbf{R}^{1/2}$ be real symmetric matrices that satisfy $\mathbf{Q}^{1/2}\mathbf{Q}^{1/2} = \mathbf{Q}$ and $\mathbf{R}^{1/2}\mathbf{R}^{1/2} = \mathbf{R}$. Using $\mathbf{u} = -\mathbf{K}\mathbf{q}$, (3) can be written as

$$\begin{aligned} &\min_{\mathbf{K}} E[\mathbf{q}^T\mathbf{Q}^{1/2}\mathbf{Q}^{1/2}\mathbf{q} + \mathbf{q}^T\mathbf{K}^T\mathbf{R}^{1/2}\mathbf{R}^{1/2}\mathbf{K}\mathbf{q}] \\ &\qquad - \mathbf{q}^T\mathbf{N}\mathbf{K}\mathbf{q} - \mathbf{q}^T\mathbf{K}^T\mathbf{N}^T\mathbf{q} \\ &\text{subject to } \dot{\mathbf{q}} = (\mathbf{A}-\mathbf{B}\mathbf{K})\mathbf{q} + \mathbf{E}\mathbf{w} \end{aligned} \tag{5}$$

Let $E[\mathbf{q}\mathbf{q}^T] = \mathbf{P}$, which is the state covariance matrix; clearly, $\mathbf{P} = \mathbf{P}^T > 0$. Utilizing the trace operator $Tr(\cdot)$ and a Lyapunov equation (the solution of which is state covariance matrix $\mathbf{P}$) to represent the stability of the system, optimization (5) can be written as

$$\begin{aligned} &\min_{\mathbf{K},\,\mathbf{P}} Tr(\mathbf{Q}^{1/2}\mathbf{P}\mathbf{Q}^{1/2}) + Tr(\mathbf{R}^{1/2}\mathbf{K}\mathbf{P}\mathbf{K}^T\mathbf{R}^{1/2}) \\ &\qquad - Tr(\mathbf{K}\mathbf{P}\mathbf{N}) - Tr(\mathbf{N}^T\mathbf{P}\mathbf{K}^T) \\ &\text{subj. to } (\mathbf{A}-\mathbf{B}\mathbf{K})\mathbf{P} + \mathbf{P}(\mathbf{A}-\mathbf{B}\mathbf{K})^T + \mathbf{E}\mathbf{E}^T = 0,\ \mathbf{P} = \mathbf{P}^T > 0 \end{aligned} \tag{6}$$

Next, consider the following problem:

$$\begin{aligned} &\min_{\mathbf{F},\,\mathbf{S}} Tr(\mathbf{Q}^{1/2}\mathbf{S}\mathbf{Q}^{1/2}) + Tr(\mathbf{R}^{1/2}\mathbf{F}\mathbf{S}\mathbf{F}^T\mathbf{R}^{1/2}) \\ &\qquad - Tr(\mathbf{F}\mathbf{S}\mathbf{N}) - Tr(\mathbf{N}^T\mathbf{S}\mathbf{F}^T) \\ &\text{subj. to } (\mathbf{A}-\mathbf{B}\mathbf{F})\mathbf{S} + \mathbf{S}(\mathbf{A}-\mathbf{B}\mathbf{F})^T + \mathbf{E}\mathbf{E}^T < 0,\ \mathbf{S} = \mathbf{S}^T > 0 \end{aligned} \tag{7}$$

where $\mathbf{S}$ is the Lyapunov matrix. It is proposed that if $\mathbf{K}_0$ and $\mathbf{P}_0$ are the solutions to (6), and $\mathbf{F}_0$ and $\mathbf{S}_0$ are the solutions to (7), then $\mathbf{K}_0 = \mathbf{F}_0$ and $\mathbf{P}_0 = \mathbf{S}_0$. Proof of this proposition is given in the Appendix.

The optimization problem (7) is not exactly in the form of the EVP (1) since it includes the multiplicative terms $\mathbf{FS}$ (*i.e.*, the objective function is not linear), and the first inequality constraint is a BMI (*i.e.*, the constraint is not convex). To convert the BMI constraint in (7) into an LMI constraint, a new variable $\mathbf{Y} = \mathbf{FS}$ and an auxiliary parameter $\mathbf{X}$ are introduced. Using the Schur complement formula and some algebra, (7) can be written as

$$\begin{aligned} &\min_{\mathbf{Y},\,\mathbf{S},\,\mathbf{X}} Tr(\mathbf{Q}^{1/2}\mathbf{S}\mathbf{Q}^{1/2}) + Tr(\mathbf{X}) - Tr(\mathbf{Y}\mathbf{N}) - Tr(\mathbf{N}^{\mathrm{T}}\mathbf{Y}^{\mathrm{T}}) \\ &\text{subject to } \mathbf{A}\mathbf{S} - \mathbf{B}\mathbf{Y} + \mathbf{S}\mathbf{A}^{\mathrm{T}} - \mathbf{Y}^{\mathrm{T}}\mathbf{B}^{\mathrm{T}} + \mathbf{E}\mathbf{E}^{\mathrm{T}} < 0, \\ &\qquad \begin{bmatrix} \mathbf{X} & \mathbf{R}^{1/2}\mathbf{Y} \\ \mathbf{Y}^{\mathrm{T}}\mathbf{R}^{1/2} & \mathbf{S} \end{bmatrix} > 0, \quad \mathbf{S} > 0 \end{aligned} \tag{8}$$

This is equivalent to the standard LQR problem defined by (3) with feedback gain given by $\mathbf{K}_0 = \mathbf{F}_0 = \mathbf{Y}_0\mathbf{S}_0^{-1}$.

III. Dissipativity Indices and Constraints

In this section, first, a formal definition of a dissipative force is stated, and several dissipativity indices are defined. Then, for each index, a matrix inequality constraint is derived for the LMI-LQR problem. Noted that, in the field of control, the term *dissipativity* is generally used to characterize a particular input–output relation of a dynamic system and, hence, is different from the mechanical definition used herein. For further information see [11]–[14].

A. Strictly Dissipative Force

Consider an external force $f(t)$, which is applied to a system at point x_0. Let $v(t)$ be the velocity of point x_0 (with positive velocity in the same direction as positive forces). $f(t)$ is called a *strictly dissipative force* if the rate of energy added to the system is negative for all $t \geq 0$. Or,

$$f(t)v(t) \leq \varepsilon(t) < 0,\ \forall t \geq 0 \Leftrightarrow f(t) \text{ is strictly dissipative} \tag{9}$$

where $\varepsilon(t)$ is a strictly negative real function. In this paper, the term *dissipative force* is used instead of *strictly dissipative force* for convenience. Note that a damper force is a strictly dissipative force.

B. Percentage of Dissipative Control Forces

The following deterministic index computes the percentage of time that the primary control force is dissipative:

$$D_{\%} = \left(1 - \frac{1}{T}\int_0^T H[u_{\mathrm{a}}v_{\mathrm{d}}]dt\right) \times 100 \tag{10}$$

where $H(\cdot)$ is the Heaviside unit step function.

C. Probability that the Control Force is Dissipative

The probability that the control force is strictly dissipative is given by [6]

$$D_{\mathrm{p}} = P[u_{\mathrm{a}}v_{\mathrm{d}}] = \frac{1}{\pi}\mathrm{acos}(\rho_{u_{\mathrm{a}}v_{\mathrm{d}}}). \tag{11}$$

$\rho_{u_{\mathrm{a}}v_{\mathrm{d}}}$ is the correlation coefficient between u_{a} and v_{d}.

D. Indices Based on the Mean Energy Flow Rate

The expected value of condition (9) is applied to the primary control force as follows:

$$\begin{aligned} &E[u_{\mathrm{a}}(t)v_{\mathrm{d}}(t)] \leq E[\varepsilon(t)] = \mu_\varepsilon(t) < 0 \\ &\qquad\qquad \Leftarrow u_{\mathrm{a}}(t) \text{ is strictly dissipative} \end{aligned} \tag{12}$$

Note that $E[u_{\mathrm{a}}v_{\mathrm{d}}] < 0$ does not necessarily mean that the control force is strictly dissipative or mostly strictly dissipative. However, it is clear that for values of $E[u_{\mathrm{a}}v_{\mathrm{d}}] \ll \mu_\varepsilon(t)$, u_{a} has a higher mean energy flow rate, which can be used as an indication of the dissipative nature of the control force. Therefore the following index is proposed:

$$D_{\mathrm{e}} = E[u_{\mathrm{a}}v_{\mathrm{d}}]. \tag{13}$$

D_{e} is called the *mean energy flow rate* in this paper.

One problem with D_{e} is that it is not unitless; *i.e.*, a large magnitude of D_{e} may be an indication of very large values of force u_{a}. To avoid this problem, a normalized index is also proposed as follows:

$$D_{\mathrm{ne}} = \frac{E[u_{\mathrm{a}}v_{\mathrm{d}}]}{\sqrt{E[u_{\mathrm{a}}^2]}\sqrt{E[v_{\mathrm{d}}^2]}}. \tag{14}$$

D_{ne} will be called the *normalized mean energy flow rate*.

In a standard LQ problem, all stochastic variables are zero-mean. Therefore, D_{ne} is the correlation coefficient between the force u_{a} and the velocity v_{d}, *i.e.*, $D_{\mathrm{ne}} = \rho_{u_{\mathrm{a}}v_{\mathrm{d}}}$.

E. Dissipativity Constraints

Among the indices given, $D_{\%}$ cannot be represented in a manner suitable for the LQR problem since it is a deterministic index. To find a constraint for D_{p}, $\rho_{u_{\mathrm{a}}v_{\mathrm{d}}}$ is represented in a form suitable for the EVP first. Let the velocity of the system at the point where the damper exerts force be given by $v = \mathbf{C}_{\mathrm{v}}\mathbf{q}$. Since the LQR control force is as $u_{\mathrm{a}} = -\mathbf{F}\mathbf{q}$, $\rho_{u_{\mathrm{a}}v_{\mathrm{d}}}$ can be written as

$$\rho_{u_{\mathrm{a}}v_{\mathrm{d}}} = \frac{E[-\mathbf{F}\mathbf{q}(\mathbf{C}_{\mathrm{v}}\mathbf{q})^{\mathrm{T}}]}{\sqrt{E[-\mathbf{F}\mathbf{q}(-\mathbf{F}\mathbf{q})^{\mathrm{T}}]}\sqrt{E[\mathbf{C}_{\mathrm{v}}\mathbf{q}(\mathbf{C}_{\mathrm{v}}\mathbf{q})^{\mathrm{T}}]}}. \tag{15}$$

Using $\mathbf{P} = E[\mathbf{q}\mathbf{q}^{\mathrm{T}}]$, a constraint for D_{p} is obtained as

$$\frac{1}{\pi}\mathrm{acos}\left(\frac{-\mathbf{F}\mathbf{P}\mathbf{C}_{\mathrm{v}}^{\mathrm{T}}}{\sqrt{\mathbf{F}\mathbf{P}\mathbf{F}^{\mathrm{T}}}\sqrt{\mathbf{C}_{\mathrm{v}}\mathbf{P}\mathbf{C}_{\mathrm{v}}^{\mathrm{T}}}}\right) > \gamma_{\mathrm{p}} \quad \text{where} \quad 0 \leq \gamma_{\mathrm{p}} \leq 1. \tag{16}$$

Using the same notation, a constraint for D_{e} is found as

$$-\mathbf{F}\mathbf{P}\mathbf{C}_{\mathrm{v}}^{\mathrm{T}} < \gamma_{\mathrm{e}} \quad \text{where} \quad \gamma_{\mathrm{e}} < \mu_\varepsilon. \tag{17}$$

Similarly, a constraint for D_{ne} is given by

$$\frac{-\mathbf{F}\mathbf{P}\mathbf{C}_{\mathrm{v}}^{\mathrm{T}}}{\sqrt{\mathbf{F}\mathbf{P}\mathbf{F}^{\mathrm{T}}}\sqrt{\mathbf{C}_{\mathrm{v}}\mathbf{P}\mathbf{C}_{\mathrm{v}}^{\mathrm{T}}}} < \gamma_{\mathrm{ne}} \quad \text{where} \quad -1 < \gamma_{\mathrm{ne}} < 1. \tag{18}$$

Clearly, the conditions given by

$$0.5 \leq \gamma_{\mathrm{p}} \leq 1, \qquad \gamma_{\mathrm{e}} < 0, \qquad -1 < \gamma_{\mathrm{ne}} < 0 \tag{19}$$

are desired as the primary control force is more likely to dissipate energy for these values.

It should be noted that the normalized mean energy flow constraint given by (18) enforces the probability constraint (16) (see Section III-D). Since (18) does not include a trigonometric function, it is more suitable for the EVP problem, and (16) is not considered further.

It is now required that the constraints (17) or (18) be represented in terms of new Lyapunov matrices, $\mathbf{S}_e$ and $\mathbf{S}_{ne}$. However, the introduction of $\mathbf{S}_e$ and $\mathbf{S}_{ne}$ requires the addition of equality constraints given by

$$\begin{aligned}(\mathbf{A}-\mathbf{BF})\mathbf{S}_e + \mathbf{S}_e(\mathbf{A}-\mathbf{BF})^T + \mathbf{E}\mathbf{E}^T = 0\\ (\mathbf{A}-\mathbf{BF})\mathbf{S}_{ne} + \mathbf{S}_{ne}(\mathbf{A}-\mathbf{BF})^T + \mathbf{E}\mathbf{E}^T = 0\end{aligned} \tag{20}$$

Moreover, since (18) is a nonlinear matrix inequality constraint, and a corresponding LMI (or, possibly, BMI) may not be available, a numerical solution of the EVP with constraint (18) is not guaranteed by the available solution techniques. Therefore, the following constraint is used:

$$-\mathbf{F}\mathbf{S}\mathbf{C}_v^T < \gamma_e^L \quad \text{where} \quad \gamma_e^L < \mu_\varepsilon . \tag{21}$$

There are several advantages and disadvantages of this constraint. First, (21) does not fully represent the indices D_e and D_{ne} since the equality constraints (20) are dropped. Also, the term $-\mathbf{F}\mathbf{S}\mathbf{C}_v^T$ is not a normalized index. In contrast, this constraint simply allows a numerical solution to this sophisticated multiobjective problem, which is the fundamental philosophy behind the LMI-EVP approach.

Dissipativity constraint (21) can be added to the LQR problem (8) for various values of μ_ε^L. The new controllers may have various dissipativity levels and can be used in a semiactive system to investigate the correlation between the dissipativity indices and the performance.

IV. A Numerical Example

The 2DOF shear building model shown in Fig. 2 is considered as the numerical example. The state-space representation of the equation of motion is straightforward and will not be given here. The floor masses m_1 and m_2 are 100 tons. The stiffnesses k_1 and k_2 are selected such that the story periods are 0.5 secs. Similarly, the story damping coefficients are found by setting the modal damping ratios to 2%. An ideal smart damper is attached between the first floor and the ground. An ideal damper is a hypothetical device that can successfully mimic the primary controller when the primary controller force is strictly dissipative; otherwise, it produces no force, *i.e.*,

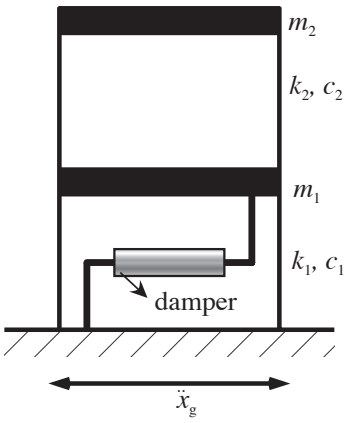

Fig. 2. The two-DOF system.

$$u_d = \begin{cases} u_a, & u_a v_d < 0 \\ 0, & u_a v_d \geq 0 \end{cases} \tag{22}$$

where u_d and v_d are the damper force and velocity, respectively, and u_a is the primary control force.

The control systems investigated are as follows:

- *Act*: This is a theoretical fully active system. A fictitious fully active actuator is used instead of a smart damper. Standard LQR is used to command the actuator.
- *Act-Dis*: This system is same as *Act* except the proposed LMI-EVP controller with the dissipativity constraint is utilized instead of the standard LQR.
- *SAct*: This is a semiactive system using a smart damper commanded by a clipped optimal control strategy. The primary controller is a standard LQR controller.
- *SAct-Dis*: This system is same as *SAct* except that the proposed LMI-EVP controller with the dissipativity constraint is used.

In the control design, the output vector to be minimized is selected as the drifts of each story and the absolute accelerations of each floor, $\mathbf{z} = [x_1 \quad x_2 - x_1 \quad \ddot{x}_1^{abs} \quad \ddot{x}_2^{abs}]^T$. The control design parameters are selected as

$$\begin{aligned}\mathbf{Q} = \mathbf{C}_z^T\tilde{\mathbf{Q}}\mathbf{C}_z, \quad \mathbf{N} = \mathbf{C}_z^T\tilde{\mathbf{Q}}\mathbf{D}_z + \mathbf{C}_z^T\tilde{\mathbf{N}},\\ \mathbf{R} = \tilde{\mathbf{R}} + \mathbf{D}_z^T\tilde{\mathbf{Q}}\mathbf{D}_z + \mathbf{D}_z^T\tilde{\mathbf{N}} + \tilde{\mathbf{N}}^T\mathbf{D}_z\end{aligned} \tag{23}$$

where

$$\tilde{\mathbf{Q}} = diag\left[\alpha\mathbf{I}_{2\times 2} \quad \frac{\beta}{\omega_n^4}\mathbf{I}_{2\times 2}\right], \quad \tilde{\mathbf{R}} = \eta \ , \quad \tilde{\mathbf{N}} = \mathbf{0} . \tag{24}$$

This set of parameters allows one to choose the relative importance of the drift and absolute acceleration responses. The normalization frequency ω_n is taken as 10.5 rad/sec; this value is found such that the drift and absolute acceleration portions of the term $E[\mathbf{z}^T\tilde{\mathbf{Q}}\mathbf{z}]$ give the same values for ($\alpha = 1$, $\beta = 1$) in active control.

A parametric study is carried out to find the (γ_e^L, R_f) pair that yields the smallest D_e for each control design where R_f is the feasibility radius. R_f is a MATLAB LMI solver parameter that sets the Eucledian norm of the solution vector. The resulting (γ_e^L, R_f) values are then employed in the dynamic analysis of the 2DOF structure excited by an artificial 50 sec white noise signal normalized by 1000. The performance of the structure is investigated using three indices:

$$J_d = \sigma_{x_1}^2 + \sigma_{x_2-x_1}^2, \quad J_a = \frac{1}{\omega_n^4}(\sigma_{\ddot{x}_1^{abs}}^2 + \sigma_{\ddot{x}_2^{abs}}^2) \tag{25}$$

$$J = J_d + \frac{\beta}{\alpha}J_a + \frac{\eta}{\alpha}\sigma_u^2 \tag{26}$$

where, for a discrete time history $x(n\Delta t)$, σ_x^2 is defined by

$$\sigma_x^2 = \frac{1}{N}\sum_{k=1}^{N}[x(k\Delta t)]^2 . \tag{27}$$

Figs. 3-5 are obtained for $\beta = 1000$ and several values of α in $[10^{-5},10^{5}]$. In all plots, the performance indices are normalized by the corresponding uncontrolled system indices. The difference in the RMS control force scales in Fig. 3 and Fig. 4 is due to the normalization of the white noise. In the discussions below, the RMS control force scale of Fig. 4 is used. The following observations are made:

- For practical control force levels ($[10^{4}, 10^{5}]$ N in Fig. 4) the dissipativity of the controller is very high for this particular structure and control design.
- The LMI method improves D_{e} and D_{ne} for a given u_{RMS}. This is more clear for $u_{RMS} \approx 10^{4.8}$ N. However, the best improvement in $D_{\%}$ is for $u_{RMS} \approx 10^{4.2}$ N. Moreover, it is observed that the LMI method improves the drift performance about 25% for $u_{RMS} \approx 10^{4.8}$ N. This improvement is not clear on the overall performance index J.
- Another difference between D_{e} and D_{ne} is that the highest value of D_{e} corresponds to RMS control force levels of $[10^{4.7}, 10^{5}]$ N, while this range is $[10^{4.1}, 10^{4.3}]$ N for D_{ne}. Also observed is the similarity between D_{ne} and $D_{\%}$
- The LMI method narrows the range of possible u_{RMS} values for the control designs. The LMI method and the dissipativity indices may give a good sense of the achievable semiactive performance, letting the designer avoid simulations that will not yield better results.

V. Conclusions

In this paper, the dissipativity and performance of semiactive systems with smart dampers are investigated. An LQR problem is defined in terms of convex LMI constraints, and a dissipativity constraint based on the mean energy flow rate of the control force is appended to the LMI-LQR problem to modify the dissipative nature of the controller. This controller is then employed in the semiactive control of a 2DOF building structure with and ideal damper as an example. It is observed that the proposed LMI approach was able to considerably improve drift performance of the controller.

Appendix

The equivalency of the problems given by (6) and (7) is proven here. In the following, $\mathbf{S} = \mathbf{S}^{T} > 0$, $\mathbf{P} = \mathbf{P}^{T} > 0$ and $\mathbf{A}$ is Hurwitz, and the following shorthand notations are used: $\mathbf{L_S} \equiv \mathbf{AS} + \mathbf{SA}^{T} + \mathbf{\Psi}$ and $\mathbf{L_P} \equiv \mathbf{AP} + \mathbf{PA}^{T} + \mathbf{\Psi}$ where $\mathbf{\Psi} = \mathbf{\Psi}^{T} > 0$.

Corollary 1 $\mathbf{S} > \mathbf{P} \Leftrightarrow \mathbf{L_S} < \mathbf{L_P}$.
Proof: $\mathbf{S} > \mathbf{P} \Leftrightarrow \mathbf{S} - \mathbf{P} > 0 \Leftrightarrow \mathbf{A}(\mathbf{S} - \mathbf{P}) + (\mathbf{S} - \mathbf{P})\mathbf{A}^{T} < 0$
$\Leftrightarrow \mathbf{AS} + \mathbf{SA}^{T} < \mathbf{AP} + \mathbf{PA}^{T} \Leftrightarrow \mathbf{L_S} < \mathbf{L_P}$.

Corollary 2 $\mathbf{L_S} < 0$ and $\mathbf{L_P} = \mathbf{0} \Rightarrow \mathbf{S} > \mathbf{P}$.
This is a consequence of corollary 1.

Corollary 3 $\mathbf{\Phi} = \mathbf{\Phi}^{T} > 0 \Rightarrow Tr(\mathbf{C\Phi C}^{T}) > 0$.
Proof: Let $\mathbf{c}_i$ be the i^{th} row of $\mathbf{C}$. Then, $\mathbf{\Phi} > 0 \Leftrightarrow \mathbf{c}_i\mathbf{\Phi}\mathbf{c}_i^{T} > 0 \ \forall i \Rightarrow \sum \mathbf{c}_i\mathbf{\Phi}\mathbf{c}_i^{T} = Tr(\mathbf{C\Phi C}^{T}) > 0$.

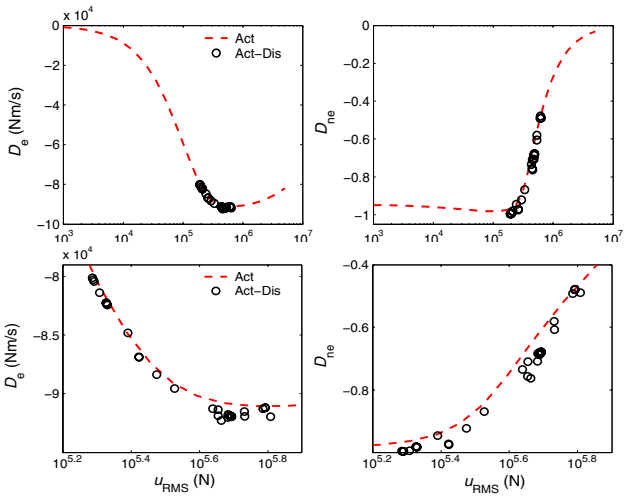

Fig. 3. D_{n} and D_{ne} plots for the 2DOF building structure from the covariance analysis (overall and detailed).

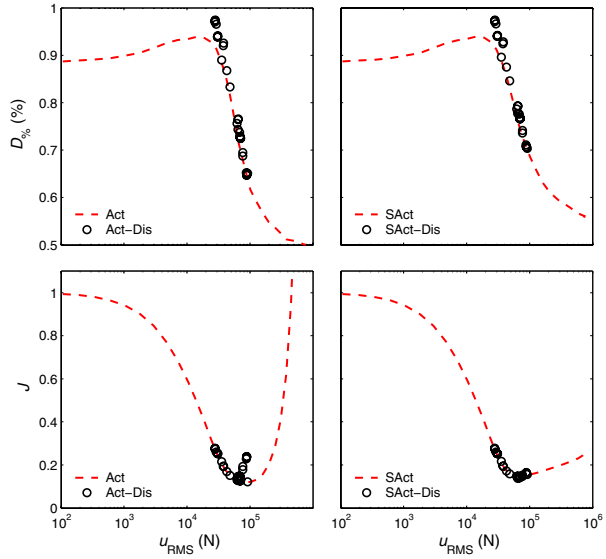

Fig. 4. $D_{\%}$ and normalized J plots for the 2DOF building structure from simulations for a white noise excitation.

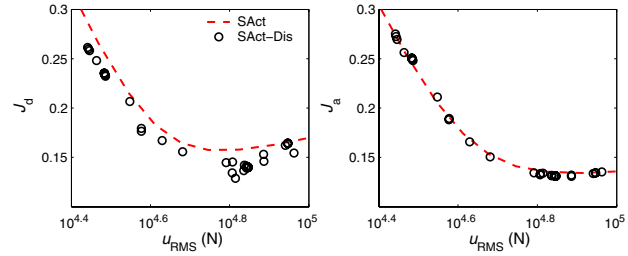

Fig. 5. Detailed plots of normalized J_{d} and J_{a} of the 2DOF building structure from simulations for a white noise excitation.

Corollary 4 $\mathbf{S} > \mathbf{P} \Rightarrow Tr(\mathbf{CSC}^{\mathrm{T}}) > Tr(\mathbf{CPC}^{\mathrm{T}})$.
Proof: $\mathbf{S} > \mathbf{P} \Leftrightarrow \mathbf{S} - \mathbf{P} > 0 \Rightarrow Tr[\mathbf{C}(\mathbf{S}-\mathbf{P})\mathbf{C}^{\mathrm{T}}] > 0 \Leftrightarrow Tr(\mathbf{CSC}^{\mathrm{T}} - \mathbf{CPC}^{\mathrm{T}}) > 0 \Leftrightarrow Tr(\mathbf{CSC}^{\mathrm{T}}) - Tr(\mathbf{CPC}^{\mathrm{T}}) > 0 \Leftrightarrow Tr(\mathbf{CSC}^{\mathrm{T}}) > Tr(\mathbf{CPC}^{\mathrm{T}})$.

Corollary 5 Let $S = \{\mathbf{S} | \mathbf{L}_{\mathbf{S}} < 0\}$; then, there exists a unique matrix $\mathbf{P}_0$ such that $\mathbf{P}_0 = [\mathbf{P} | \mathbf{L}_{\mathbf{P}} = 0]$ and $\mathbf{P}_0 < \mathbf{S}$ for any $\mathbf{S} \in S$. Moreover, $Tr(\mathbf{CP}_0\mathbf{C}^{\mathrm{T}}) < Tr(\mathbf{CSC}^{\mathrm{T}})$ holds for any $\mathbf{S} \in S$.
Proof: See corollaries 2 and 4.

Lemma 6 Let

$$\mathbf{S}_0 = \arg \min_{\mathbf{S}} Tr(\mathbf{CSC}^{\mathrm{T}}) \text{ subject to } \mathbf{L}_{\mathbf{S}} \le 0 \quad \text{and} \quad \mathbf{P}_0 = [\mathbf{P} | \mathbf{L}_{\mathbf{P}} = 0]. \tag{A.1}$$

Then, $\mathbf{S}_0 = \mathbf{P}_0$ and $Tr(\mathbf{CS}_0\mathbf{C}^{\mathrm{T}}) = Tr(\mathbf{CP}_0\mathbf{C}^{\mathrm{T}})$.
Proof: The proof is readily obtained using corollary 5.

Theorem 7 The problems (6) and (7) are equivalent.
Proof: It can be shown with some matrix algebra that the objective function in the LQR problem can be written as

$$Tr(\mathbf{Q}^{1/2}\mathbf{PQ}^{1/2}) + Tr(\mathbf{R}^{1/2}\mathbf{KPK}^{\mathrm{T}}\mathbf{R}^{1/2}) - Tr(\mathbf{KPN}) - Tr(\mathbf{N}^{\mathrm{T}}\mathbf{PK}^{\mathrm{T}}) = Tr[\mathbf{C}_{\underline{z}}(\mathbf{K})\mathbf{P}\mathbf{C}_{\underline{z}}^{\mathrm{T}}(\mathbf{K})] \tag{A.2}$$

where

$$\mathbf{C}_{\underline{z}}(\mathbf{K}) = \begin{bmatrix} \mathbf{Q}^{1/2} - \boldsymbol{\Upsilon}\mathbf{K} \\ \boldsymbol{\Upsilon}^{\mathrm{T}} - \mathbf{R}^{1/2}\mathbf{K} \end{bmatrix} \tag{A.3}$$

for real symmetric matrices $\mathbf{Q}^{1/2}$ and $\mathbf{R}^{1/2}$. Note that there is not necessarily a unique $\boldsymbol{\Upsilon}$ for a given $\mathbf{N}$ in (A.2). The gain in problem (6) can be found as

$$\mathbf{K}_0 = \arg \min_{\mathbf{K}} Tr[\mathbf{C}_{\underline{z}}(\mathbf{K})\mathbf{P}_0(\mathbf{K})\mathbf{C}_{\underline{z}}(\mathbf{K})] \tag{A.4}$$

where

$$\mathbf{P}_0(\mathbf{K}) = [\mathbf{P} \mid \mathbf{A}_{\mathrm{c}}(\mathbf{K})\mathbf{P} + \mathbf{P}\mathbf{A}_{\mathrm{c}}^{\mathrm{T}}(\mathbf{K}) + \mathbf{E}\mathbf{E}^{\mathrm{T}} = 0] \quad \text{and} \quad \mathbf{A}_{\mathrm{c}}(\mathbf{K}) = \mathbf{A} - \mathbf{B}\mathbf{K}. \tag{A.5}$$

Similarly, the gain in problem (7) can be written as

$$\mathbf{F}_0 = \arg \min_{\mathbf{F}} Tr[\mathbf{C}_{\underline{z}}(\mathbf{F})\mathbf{S}_0(\mathbf{F})\mathbf{C}_{\underline{z}}(\mathbf{F})] \tag{A.6}$$

where

$$\mathbf{S}_0(\mathbf{F}) = \arg \min_{\mathbf{S}} Tr[\mathbf{C}_{\underline{z}}(\mathbf{F})\mathbf{S}\mathbf{C}_{\underline{z}}^{\mathrm{T}}(\mathbf{F})] \text{ subject to } \mathbf{A}_{\mathrm{c}}(\mathbf{F})\mathbf{S} + \mathbf{S}\mathbf{A}_{\mathrm{c}}^{\mathrm{T}}(\mathbf{F}) + \mathbf{E}\mathbf{E}^{\mathrm{T}} < 0 \text{ and } \mathbf{A}_{\mathrm{c}}(\mathbf{F}) = \mathbf{A} - \mathbf{B}\mathbf{F}. \tag{A.7}$$

Using Lemma 6, one can show that the matrix functions given by equations (A.5) and (A.7) are equal. Therefore, $\mathbf{K}_0 = \mathbf{F}_0$ and $\mathbf{P}_0(\mathbf{K}_0) = \mathbf{S}_0(\mathbf{F}_0)$.

REFERENCES

[1] M. D. Symans and M. C. Constantinou, "Semi-active control systems for seismic protection of structures: A state-of-the-art review," *Engineering Structures*, vol. 21, no. 6, 1999, pp. 469–487.

[2] T. T. Soong and B. F. Spencer Jr., "Supplemental energy dissipation: State-of-the-art and state-of-the-practice," *Engineering Structures*, vol. 24, no. 3, 2002, pp. 243–259.

[3] S. J. Dyke, B. F. Spencer Jr., M. K. Sain and J. D. Carlson, "Modeling and control of magnetorheological dampers for seismic response reduction," *Smart Mat'ls & Structs.*, vol. 5, no. 5, 1996, pp. 565–575.

[4] B. Erkus, M. Abé and Y. Fujino, "Investigation of semi-active control for seismic protection of elevated highway bridges," *Engineering Structures*, vol. 24, no. 3, 2002, pp. 281–293.

[5] J. C. Ramallo, E. A. Johnson and B. F. Spencer Jr., "'Smart' base isolation systems," *Journal of Engineering Mechanics*, ASCE, vol. 128, no. 10, 2002, pp. 1088–1099.

[6] J. A. Inaudi, "Performance of variable-damping systems: Theoretical Analysis and Simulation," in *Proceedings of 3rd International Workshop on Structural Control*, Paris, France, 2000, pp. 301–316.

[7] S. Boyd, L. E. Ghaoui, E. Feron and V. Balakrishnan, *Linear Matrix Inequalities in System and Control Theory*, Studies in Applied Mathematics, vol. 15, SIAM, Philadelphia, Pennsylvania, 1994.

[8] J. N. Yang, S. Lin and F. Jabbari, "Linear Multiobjective Control Strategies for Wind-Excited Buildings," *Journal of Engineering Mechanics*, ASCE, vol. 130, no. 4, 2004, pp. 471–477.

[9] Y. Nesterov and A. Nemirovskii, *Interior-point Polynomial Algorithms in Convex Programming*, Studies in Applied Mathematics, vol. 13, SIAM, Philadelphia, Pennsylvania, 1994.

[10] P. Gahinet, A. Nemirovski, A. J. Laub and M. Chilali, *LMI Control Toolbox*. MathWorks, Natick, Massachusetts, 1995.

[11] M. E. Gurtin and I. Herrera, "On dissipation inequalities and linear viscoelasticity," *Division of Applied Mathematics Technical Report Nonr-562(25)/27*, Brown University, Providence, Rhode Island, 1964.

[12] J. C. Willems, "Dissipative dynamical systems – Part I: General theory," *Archive for Rational Mechanics and Analysis*, vol. 45, no. 5, 1972, pp. 321–351.

[13] J.C. Willems, "Dissipative dynamical systems – Part II: Linear systems with quadratic supply rates," *Archive for Rational Mechanics and Analysis*, vol. 45, no. 5, 1972, pp. 352–393.

[14] J. T. Wen, "Time domain and frequency domain conditions for strict positive realness," *IEEE Transactions on Automatic Control*, vol. 33, no. 10, 1988, pp. 988–992.

[15] G. E. Dullerud and F. Paganini, *A Course in Robust Control Theory: A Convex Approach*, Springer, New York, 2000.

[16] C. Scherer, P. Gahinet and M. Chilali, "Multiobjective output-feedback control via LMI optimization," *IEEE Transactions on Automatic Control*, vol. 42, no. 7, 1997, pp. 896–911.

[17] J. C. Willems, "Least squares stationary optimal control and the algebraic Ricatti equation," *IEEE Transactions on Automatic Control*, vol. AC-16, no. 6, 1971, pp. 621–634.

[18] P. P. Khargonekar and M. A. Rotea, "Mixed H_2/H_∞ control: A convex optimization approach," *IEEE Transactions on Automatic Control*, vol. 36, no. 7, 1991, pp. 824–837.

[19] E. Feron, V. Balakrishnan, S. Boyd and L. El Ghaoui, "Numerical methods for H_2 related problems," in *Proceedings of American Control Conference*, Chicago, Illinois, 1992, pp. 2921–2922.

[20] L. Turan, M. G. Safonov and C. H. Huang, "Synthesis of positive real feedback systems: A simple derivation via Parrott's theorem," *IEEE Trans. on Automatic Control*, vol. 42, no. 8, 1997, pp. 1154–1157.